Oral biofilm dysbiosis during experimental periodontitis

Apoena Aguiar Ribeiro[1], Yizu Jiao[2], Mustafa Girnary[2], Tomaz Alves[2], Liang Chen[2], Anna Farrell[1], Di Wu[3], Flavia Teles[4], Naohiro Inohara[5], Karen V. Swanson[6], Julie T. Marchesan[2]

1. Division of Diagnostic Sciences (Microbiology and Cariology), Adams School of Dentistry, University of North Carolina, Chapel Hill, USA
2. Division of Comprehensive Oral Health (Periodontology), Adams School of Dentistry, University of North Carolina at Chapel hill, Chapel Hill, NC, USA
3. Division of Oral and Craniofacial Health Sciences, School of Dentistry, University of North Carolina, Chapel Hill, USA. Department of Biostatistics, Gillings School of Global Public Health, University of North Carolina, Chapel Hill, USA.
4. Department of Basic & Translational Sciences, Penn Dental Medicine, University of Pennsylvania
5. Department of Pathology, Michigan Medicine, University of Michigan
6. Division of Infectious Diseases, School of Medicine, University of North Carolina, Chapel Hill, NC, USA

Acknowledgements

The authors would like to thank the following support funding agency/grant numbers T90DE021986 and F32DE026688 (to YJ), K01DE027087 (to JTM), R01AI153265 (to KVS), R01DE023836 (to SO) and the Fulbright/CAPES program finance code 001 (to TA). The UNC Microbiome Core, which is funded in part by the Center for Gastrointestinal Biology and Disease (CGIBD P30 DK034987) and the UNC Nutrition Obesity Research Center (NORC P30 DK056350). The authors would like to thank the late Dr. Steven Offenbacher for his guidance and support during the development of this study. The authors declare no potential conflicts of interest with respect to the authorship and/or publication of this article.

This is the author manuscript accepted for publication and has undergone full peer review but has not been through the copyediting, typesetting, pagination and proofreading process, which may lead to differences between this version and the Version of Record. Please cite this article as doi: 10.1111/omi.12389.

Abstract

Objectives: We have previously characterized the main osteoimmunological events that occur during ligature periodontitis. This study aims to determine the polymicrobial community shifts that occur during disease development.

Methods: Periodontitis was induced in C57BL/6 mice using the ligature-induced periodontitis model. Healthy oral mucosa swabs and ligatures were collected every 3-days from 0 to 18 days post-ligature placement. Biofilm samples were evaluated by 16SrRNA gene sequencing (Illumina MiSeq) and QIIME. Timecourse changes were determined by relative abundance, diversity, and rank analyses (PERMANOVA, Bonferroni-adjusted).

Results: Microbial differences between health and periodontal inflammation were observed at all phylogenic levels. An evident microbial community shift occurred in 25 genera during the advancement of "gingivitis" (3-6d) to periodontitis (9-18d). From day 0-18, dramatic changes were identified *Streptococcus* levels, with an overall decrease (54.04-0.02%) as well an overall increase of *Enterococcus* and *Lactobacillus* (23.7-73.1% and 10.1%-70.2%, respectively). Alpha-diversity decreased to its lowest at 3d, followed by an increase in diversity as disease advancement. Beta-diversity increased after ligature placement, indicating that bone loss develops in response to a greater microbial variability (p=0.001). Levels of facultative and strict anaerobic bacteria augmented over the course of disease progression, with a total of 8 species significantly different during the 18-day period.

Conclusion: The data supports that murine gingival inflammation and alveolar bone loss develop in response to microbiome shifts. Bacterial diversity increased during progression to bone loss. These findings further support the utilization of the periodontitis ligature model for microbial shift analysis under different experimental conditions.

Keywords: dysbiosis, experimental periodontitis, biofilm

Corresponding author

Julie Marchesan

Division of Comprehensive Oral Health (Periodontology)

University of North Carolina at Chapel Hill - Adams School of Dentistry

3506 Koury Oral Health Sciences Building

Chapel Hill, NC 27599-7455
email: julie_marchesan@unc.edu

INTRODUCTION

Periodontitis is an inflammatory disease caused by a dysbiotic microbiota (Abe, Hajishengallis, 2013). The dysbiosis is characterized by the microbial shift that occurs in the biofilm with a decrease in the number of beneficial symbionts and/or an increase in the number of pathobionts, as microorganisms become pathogenic when host-microbe homeostasis breaks down (Jiao et al 2013, Hajishengallis, Lamont 2016). The polymicrobial community shift induces a host response that results in the destruction of the connective tissue and alveolar bone supporting the tooth. In the clinical setting, individuals with periodontal disease consistently demonstrate a shift in biofilm microbial composition compared to healthy individuals, including increased abundances of certain phylotypes (Paster et al 2001, Griffen et al 2012, Paes Batista da Silva et al 2016, Marchesan et al 2016).

To better understand the microbial changes and inflammatory host-response to these changes, it is important to explore the etiology of periodontitis to improve its treatment. Many host and environmental factors are associated with an oral microbiota dysbiosis, including increased microbial challenge (e.g. biofilm load), smoking and systemic diseases (Teles et al 2021, Sanz et al 2018, Nociti et al 2015). Although human biofilm samples can be used to characterize the difference between healthy and disease states, dynamic microbial shifts cannot be fully investigated in the clinical setting. Moreover, neither the direct cause nor effect of different host and environmental factors that can directly induce a microbial shift related to disease can be explored in humans. Therefore, experimental animal models are a powerful platform to complement results derived from clinical studies (Hajishengallis et al 2015, Wu et al. 2016).

Different models have been used to study periodontal disease in mice, including the oral gavage, chamber model and ligature models (Graves et al. 2018). Ligature-induced periodontitis in mice have long served as an animal model for periodontitis. We previously demonstrated that there are distinct osteo-immunological events that developed from health to gingival inflammation and transition to periodontitis at 18 days post-ligature placement (Marchesan et al. 2018). While it is known that bone loss in this model develops in response to bacterial presence, information on the composition and microbial shifts of their oral microbiota is limited. Therefore, the purpose of this study was to expand on our previous immune findings (Marchesan et al. 2018) and characterize microbiota changes that occur during periodontitis development in a time-dependent manner. We hypothesized that the ligature placement would be accompanied by time-dependent shift of microorganisms, that can be associated with inflammation and periodontal disease development.

METHODS

Periodontitis murine model

The protocol was approved by the by University of North Carolina-Chapel Hill Institutional Animal Care & Use Committee and can be observed in Figure 1. Twenty-eight C57BL/6 wild-type, specific pathogen-free (SPF) female mice aged 8-10 weeks were purchased from Taconic Biosciences. Mice were acclimatized to the animal facility (under pathogen-free conditions) for a period of 7 days upon arrival, and 4 mice were randomly assigned to one of the groups associated by the time-course of the study period. Experimental periodontitis was induced using the ligature model as previously described by our group (Marchesan et al 2018). Briefly, sterile silk sutures (5-0, SUT-15-1, Roboz Surgical Instrument, Gaithersburg, MD, USA) knotted ~2.5mm apart were placed between the first and second maxillary molars using a ligature holder while the mouse was under sedation with isoflurane. Mice were evaluated every 3 days from health (baseline) to 18 days post-ligature placement. Ligature and plaque samples were collected for further analysis in accordance with previous publications (Marchesan et al 2012, Marchesan et al 2013, Jiao et al 2013). For baseline collection, a sterile swab was placed in the oral cavity of mice and swirled for 15s before being placed in sterile PBS (Thermo Fisher Scientific, cat. no. 14190144). Tubes were centrifuge for 5 minutes at 13,000 RPM at 4°C. After centrifugation, PBS was discarded, and samples were stored at -80°C until analysis. At the additional experimental timepoints, ligatures were collected with the usage of a sterile fine-point forceps (Fisher, cat. no. 16-100-113). Collected ligatures were placed in an Eppendorf tube and stored at −80°C. Samples were excluded from the analysis if a ligature was lost before the end point of the experiment. If lost, no ligature was replaced in the mouse to allow the development of a microbial shift. Microbiota analysis was conducted after confirmation of bone destruction by μCT and histological analysis, which was previously conducted and published (Marchesan et al 2018).

DNA isolation and 16s rRNA amplicon library preparation and sequencing

DNA isolation, preparation of sequencing libraries and sequencing were done in the UNC Microbiome Core Facility as described (Jones et al. 2018). Briefly, bacterial DNA extraction was performed using QIAmp DNA extraction kit (QIAGEN). A step of pre-incubation with lysozyme for 30 min was introduced to the protocol to ensure optimal DNA yield from Gram-positive bacteria.

For generation of sequencing libraries, 12.5ng of total DNA from each sample was amplified using the 2x KAPA HiFi HotStart ReadyMix (KAPA Biosystems, Wilmington, MA). Primers targeting the V3–V4 region of the 16S rRNA gene (Edwards et al. 1989; Thompson et al. 2015) were designed to incorporate Illumina compatible sequencing adaptors. The complete sequences of the primers were: 515 F – 5' TCGTCGGCAGCGTCAGATGTGTATAAGAGACAGGTGCCAGCMGCCGCGGTAA 3'; 806 R – 5'GTCTCGTGGGCTCGGAGATGTGTATAAGAGACAGGGACTACHVGGGTWTCTAAT 3'. PCR conditions consisted of an initial denaturing step at 95˚ for 3 min, 25 cycles of 95˚C for 30 sec, 55˚C for 30 sec and 72˚C for 30 sec, followed by extension at 72˚C for 5 min and a final hold at 4˚C. Illumina sequencing adapters and dual index barcodes (Illumina, San Diego, CA) were added using one more round of PCR amplification consisting of 8 cycles. PCR products were purified using AMPure XP reagent (Beckman Coulter, Indianapolis, IN), quantified by Quanti-IT Picogreen dsDNA 1 kit (Invitrogen) and pooled in equimolar amounts. Sequencing was performed on a MiSeq instrument (Illumina) operating Real Time Analysis software version 1.17.28. Paired-end sequencing used custom primers and a 500-cycle sequencing kit (version 3) according to manufacturer instructions. Amplicon sequencing was carried out in the presence of 7% PhiX control (Illumina) to allow proper focusing and matrix calculations.

Bioinformatics pipeline and statistical analysis

Raw sequencing data files were processed using the open-source software pipeline Quantitative Insights into Microbial Ecology (QIIME) version 1.8 (Caporaso et al. 2010). Barcode and primer trimming and sequence quality filtering was performed using QIIME's default script settings. Operational taxonomic units (OTUs) were clustered using QIIME implementation of UCLUST. Taxonomic assignment of OTUs was performed using BLAST against the Greengenes 16S rRNA database. After examining read counts, rarefaction analysis was performed a sampling depth of 10,000 sequences and rarefaction curves were plotted. Summary of taxonomic assignments were plotted as bar charts using QIIME. Observed species richness, as well as phylogenetic and non-phylogenetic alpha diversity metrics (Chao1 and Shannon's index, respectively) were recorded and compared at the 10,000 rarefaction depth. Phylogenetic and non-phylogenetic beta diversity matrices were calculated by Three-dimensional Principal Coordinate Analysis (PCoA) plots, calculated within QIIME using weighted and unweighted UniFrac distances between samples. Statistical analysis was performed with SAS 9.4 software after correction (Bonferoni-adjusted 0.006). The sequencing data will be made available when requested.

Paired t-test (within-tooth analysis) was performed to compare alpha diversity. Finally, Benjamini–Hochberg procedure for false discovery rate (Benjamini, Hochberg, 1995) and family-wise error rate (FWER; Hochberg, Benjamini, 1990) methods were applied to the p-values of the stratified MH mean score statistics for exploratory and confirmatory testing, respectively, to identify any statistically significant differences among genera. An overall error rate of 0.05 was used in each procedure.

RESULTS

After the study period, one sample from time 0 was not included due to low DNA yield, leading to a total of 27 biofilm samples (3 samples from baseline and 4 samples from each group in the time course). A total of 2,856,260 sequences were generated from the 27 biofilm samples, and matched 141 unique species. Amplicon reads with relative abundances higher than 0.01% were assigned to 7 bacterial phyla, 19 classes, 33 orders, 45 families, and 113 genera. The most frequent phyla were Bacillota (formerly Firmicutes, relative abundance ranging between 59.7% and 99.8%) and Pseudomonadota (formerly Proteobacteria, relative abundance ranging between 40.2% and 0.05%). Figure 2A shows the 20 most abundant bacterial genera and species profile distribution, according to time points, representing between 89% and 99% of the total community. The full list of bacterial samples and its OTUs can be verified in Supplemental Table 1.

Bacterial microbiome composition shifts according to time.

Bacillota encompassed the majority of sequences throughout all time courses, although an increase in Pseudomonadota was observed after 9 days (Supplemental figure 1). Among the top 10 most abundant genera, *Lactobacillus, Streptococcus*, and *Enterococcus* presented the greatest shifts in abundance during the time course and disease development (Figure 2B). *Tanerella* initially colonized at 3d with 0.8% of total bacteria, and colonization fell over the 18d (Figure 2B). The 18d time course significantly changed the community profile abundances among 8 species (Figure 2C). *Cutibacterium acnes*, *Bacteroides sp*., *B. heparinolyticus*, *Corynebacterium sp.*, *Lysinibacillus fusiformis*, *Acinetobacter lwoffii* and *Prevotella sp*. significantly decreased in abundance associated over the 18d time course, while *Staphylococcus sp*. became highly abundant by day 6, when compared with the baseline and with the other time points. Alpha diversity was highest at health (0d, pre-ligature), and decreased to its lowest level at the initial phase of disease of 3d post-ligature placement. This indicates that the microbiome becomes less diverse and, therefore, more specific to the development of periodontal inflammation (Shannon index, Paired t-test, Figure 3A). The decrease in species diversity within the ligature samples never returned to the baseline levels. Principal Coordinate Analysis (PCoA) of unweighted UniFrac showed that samples from baseline represented a very distinct community when compared with the other samples, forming a well-defined cluster (Figure 3B), with overall statistically significant differences between the microbiome communities (Pairwise PERMANOVA, p=0.001; Figure 3C). Biofilm community composition from baseline was significantly different when compared to 3 days (p=0.04), 6 days (p=0.05), 12 days (p=0.03) and 15 days (p=0.02). Other significant differences in bacterial beta diversity were found between 3 and 12 days (p=0.01), and between 9 and 12 days (p=0.02).

Community shifts associated with disease development.

In our previous study the transition from health to gingival inflammation and no bone loss occurred during the period of 3-6 days, which was dominated by innate immune events (Marchesan et al 2017). Development of gingival inflammation was followed by the progression to periodontal bone loss, which was dominated by an adaptive immune response and bone loss (Marchesan et al 2017). Considering this time course, the microbiome data analysis was stratified from days 3 and 6 were combined as an early lesion of gingival inflammation, while the data from days 9 to 18 were combined as periodontitis.

The experimental model showed differences in bacterial genera and species abundances from biofilms associated with ligature placement during gingival inflammation and periodontitis development, as can be observed in Figure 4A. Comparison of samples between experimental timelines showed that biofilms harvested at the gingival inflammation stage (3 and 6 days) had lower Shannon diversity indices than the baseline, indicating a decrease in bacterial community diversity within the samples (Figure 4B). This shift was followed by an increased diversity from gingival inflammation to periodontitis (9 to 18 days). Principal Coordinate Analysis (PCoA) of unweighted UniFrac showed that samples from baseline (Day 0) represented a very distinct community when compared with samples from gingival inflammation and periodontitis stages, which also formed well-defined clusters associated with periodontal clinical diagnosis (Figure 4C). Biofilm community beta diversity from day 0 was significantly different when compared to the community associates with gingival inflammation and periodontitis (Pairwise PERMANOVA, p=0.02 and p=0.00, respectively; Figure 4D). Biofilm community from “gingivitis” samples were also significantly diverse from periodontitis samples (Pairwise PERMANOVA, p=0.02 Figure 4D).

Figure 5A shows a clear distinction among the 20 top ranked species across all clinical diagnosis. Significant species associated with a healthy periodontium were *Cutibacterium acnes, Bacteroides sp., B. heparinolyticus, Acinetobacter lwoffii, Lysinibacillus fusiformis, Rhizobiales sp.* and *Prevotella sp*. Interestingly, the last three species were completely absent in both "gingivitis" and periodontitis statuses. *Staphylococcus sp.* was significantly associates with gingival inflammation with no bone loss, and *Erysipelotrichaceae* was associated with both diseased stages, gingival inflammation and periodontitis (Figure 5B).

Discussion

This is the first study that reports the oral microbiota shift that occurs during the development and progression of ligature-induced periodontitis. Using a high throughput method, we found that there were multiple changes in the colonization of the ligature that included anaerobic species. Similar to human disease findings, we identified an increased microbiota diversity during the transition from gingival inflammation to periodontal bone destruction. These results further support the utilization of the ligature model for microbial shift analysis under different experimental conditions.

Previous studies used a variety of murine models to explore the mechanism of periodontitis and the effectiveness of new treatments. Among these models, the ligature-induced periodontitis model shows host-bacteria interactions, acute alveolar bone loss and gingival tissue inflammation by 7-9 days (Graves et al. 2008, Marchesan et al 2018, Abe, Hajishengallis, 2013, Jiao et al. 2013). However, no study has reported a detailed analysis of oral microbiota shifts from health to a dysbiotic state in ligature periodontitis. In this study, we used 16S rRNA gene sequencing of the biofilm microbiota attached to ligatures and identified the presence of 7 microbial phyla, with the majority of the composition encompassed by Bacillota and Pseudomonadota. These findings are consistent with other literature reports that have utilized pyrosequencing (Chun et al. 2010) and DGGE (Jiao et al. 2013). In relation to bacterial shift in the biofilm, we identified an increase in Pseudomonadota induced by periodontitis. Previous studies investigated the microbiome shift associated with increases in pathogenicity, using diabetic mice, and verified that higher levels of Pseudomonadota *(Enterobacteriaceae)* and Bacillota *(Enterococcus, Staphylococcus, and Aerococcus)* were associated with infectious processes, periodontitis, and delayed wound healing (Grice et al., 2010; Souto and Colombo, 2008; Colombo et al., 2016, Demmer et al., 2017). Recent studies show an increase in oral Enterobacteriaceae with ligature-induced periodontitis development, which also agrees with our findings (Kitamoto et al 2020). Overall, our current study further demonstrated that the Pseudomonadota phylum is positively associated with murine periodontitis progression.

Among the signatures from the microbiome shift time course during biofilm development stages, our data reveals an inversely proportional relationship between a high abundance of *Streptococci* in the early stage versus the progressive increase of *Enterococci* and *Lactobacilli* towards the biofilm maturation. In agreement with previous findings (Sato et al 2021), we found that some species are associated with gingival health, including Staphylocccus and Corybacterium. Interestingly, Corybacterium is also associated with a healthy oral microbiome in humans (Paster et al 2001). As disease developed in mice, the higher *Streptococcus* prevalence on plaque outset composition was identified in our data corroborates with previous murine studies (Hasegawa et al 2006, 2010, Jiao et al 2013). These findings show the importance of this bacteria as a commensal colonizer and early dental biofilm colonizer in the oral cavity, possibly due to its adhesion properties to the hard cemento-enamel structures through the secretion of glycoproteins (Teles et al. 2012, Socransky et al., 1977). These findings are translationally consistent with *in vivo* previous results from our group where non mature ligature-induced biofilm in an experimental murine model presented enhanced abundance for *Streptococcus gordonii*. In fact, a recent human study revealed that *Streptococcus* sp. presence during early onset periodontal disease is consistent among individuals and has the potential to be considered as an early-stage microbial biomarker (Palmer et al. 2017). We identified an increase in levels of *Enterococcus* in the presence of ligature-induced periodontitis, which agrees with previous reports (Sato et al 2021). The inter-relationship between dysbiosis of the subgingival microbiome and periodontitis has been investigated by cohort studies in humans (Deng et al. 2017, Szafranski et al. 2015) and postulated the role of the microbiome on the onset and progression of periodontitis in humans. The red complex pathogen *P. gingivalis* was identified as the best marker for periodontitis, followed by *Tannerella spp.*, Treponema spp., *Fusobacterium_nucleatum_ss_vincentii_HOT_200_V1-2_3*, and *Eubacterium_XI_[G-6]_sp_V1-2_55.* Among the species that showed significant shifts during the time course, *Cutibacterium acnes* (formerly known as *Propionibacterium acnes*) are gram-positive anaerobic bacilli that are considered commensal bacteria on the skin and, in the oral cavity, has been linked to apical periodontitis in teeth with an existing root canal treatment (Niazi et al. 2010). *Bacteroides heparinolyticus* is a Gram-negative anaerobic rod isolated from humans with periodontitis (Okuda et al. 1985). *C*orynebacterium dentalis sp. nov. are Gram-positive rods that has been isolated from the dental plaque sample from periodontitis (Benabdelkader et al. 2019). *Lysinibacillus fusiformis* is a gram-positive, rod-shaped bacterium detected for the first time in the root canals. This specie produces EPS (extracellular polysaccharides) in response to environmental factors (Mahendran et al. 2013). *Acinetobacter lwoffii*, formerly known as *Mima polymorpha* or *Acinetobacter calcoaceticus var. lwoffii*, is a non-fermentative Gram-negative bacillus frequently associated with respiratory diseases and nosocomial infections due to their rapid development of multi-drug resistance, surviving desiccation and persistence in the environment for long periods of time. This pathogen have also been associated with treatment failure in patients with refractory periodontitis (Colombo et al. 1998, 2009, Souto et al. 2014).

Our study identified that ligature-induced periodontitis is associated with microbial dysbiosis, with shifts occurring from health to inflammation, and inflammation to bone destruction. These strengthens the importance of further understanding the microbiota changes that occur with the development of murine periodontitis, which may impact systemic diseases. Murine studies have shown that *P. gingivalis*-induced periodontitis increases both the development and severity of collagen-induced arthritis (Marchesan et al 2013). Recent data indicates that this is mediated by the oral-gut microbiome (Sato et al. 2017). Importantly, it shows that the oral microbiome has significant impact in the gut microbial composition (Sato et al. 2017). Enterobacteriaceae, a family that we found increased with ligature-periodontitis development, was recently shown to accumulate in the gut and lead to colitis after murine periodontitis development (Kitamoto et al 2020). Therefore, expanding our understanding of the oral microbiome composition is crucial to improve both oral and general health.

In conclusion, this is the first study that reports the shift in microbiome community during periodontitis development, using a combination of the ligature model and “high throughput method”. These findings support the utilization of the ligature model for microbial shift analysis under different experimental conditions. Future investigation building on our current study may assist to explore the underlying mechanism between host or environmental factors and microbial dysbiosis in vivo.

REFERENCES

1. Abe, T.; Hajishengallis, G. Optimization of the ligature-induced periodontitis model in mice. J. Immunol. Methods 2013, 394, 49–54.
2. Benabdelkader S, Boxberger M, Lo CI, Aboudharam G, La Scola B, Fenollar F. Corynebacterium dentalis sp. nov., a new bacterium isolated from dental plaque of a woman with periodontitis. New Microbes New Infect. 2019;33:100625.
3. Benjamini Y, Hochberg Y. Controlling the False Discovery Rate: A Practical and Powerful Approach to Multiple Testing. Journal of the Royal Statistical Society: Series B (Methodological) 1995;57:289-300.

4. Caporaso JG, Kuczynski J, Stombaugh J, et al. QIIME allows analysis of high-throughput community sequencing data. Nat Methods. 2010;7(5):335-336. doi:10.1038/nmeth.f.303
5. Chun J, Kim KY, Lee JH, Choi Y. The analysis of oral microbial communities of wild-type and toll-like receptor 2-deficient mice using a 454 GS FLX Titanium pyrosequencer. BMC Microbiol 2010;10:101.
6. Colombo AP, Haffajee AD, Dewhirst FE, Paster BJ, Smith CM, Cugini MA, et al. Clinical and microbiological features of refractory periodontitis subjects. J Clin Periodontol. 1998;25:169–180.
7. Colombo AP, Teles RP, Torres MC, Souto R, Rosalem WJ, Mendes MC, et al. Subgingival microbiota of Brazilian subjects with untreated chronic periodontitis. J Periodontol. 2002;73:360–369.
8. Demmer RT, Breskin A, Rosenbaum M, Zuk A, LeDuc C, Leibel R, Paster B, Desvarieux M, Jacobs DR Jr, Papapanou PN. The subgingival microbiome, systemic inflammation and insulin resistance: The Oral Infections, Glucose Intolerance and Insulin Resistance Study. J Clin Periodontol. 2017;44(3):255-265.
9. Deng K, Ouyang XY, Chu Y, Zhang Q. Subgingival Microbiome of Gingivitis in Chinese Undergraduates. Chin J Dent Res. 2017;20(3):145-152.
10. Edwards U., Rogall T, Blocker H, Emde M, Bottger EC. Isolation and direct complete nucleotide determination of entire genes. Characterization of a gene coding for 16S ribosomal RNA. Nucleic Acids Res. 1989;17(19):7843–53. PMID: 2798131
11. Graves, D.T.; Fine, D.; Teng, Y.-T.A.; Van Dyke, T.E.; Hajishengallis, G. The use of rodent models to investigate host-bacteria interactions related to periodontal diseases. J. Clin. Periodontol. 2008, 35, 89–105.
12. Grice EA, Snitkin ES, Yockey LJ, Bermudez DM; NISC Comparative Sequencing Program, Liechty KW, Segre JA. Longitudinal shift in diabetic wound microbiota correlates with prolonged skin defense response. Proc Natl Acad Sci U S A. 2010 Aug 17;107(33):14799-804. doi: 10.1073/pnas.1004204107. Epub 2010 Jul 28. Erratum in: Proc Natl Acad Sci U S A. 2010 Oct 12;107(41):17851.
13. Griffen AL, Beall CJ, Campbell JH, et al. Distinct and complex bacterial profiles in human periodontitis and health revealed by 16S pyrosequencing. ISME J 2012;6:1176-1185.
14. Hajishengallis G, Lamont RJ, Graves DT. The enduring importance of animal models in understanding periodontal disease. Virulence 2015;6:229-235.
15. Hajishengallis G, Lamont RJ. Dancing with the Stars: How Choreographed Bacterial Interactions Dictate Nososymbiocity and Give Rise to Keystone Pathogens, Accessory Pathogens, and Pathobionts. Trends Microbiol 2016;24:477-489.
16. Hasegawa M, Yang K, Hashimoto M, Park JH, Kim YG, Fujimoto Y, Nuñez G, Fukase K, Inohara N. Differential release and distribution of Nod1 and Nod2 immunostimulatory molecules among bacterial species and environments. J Biol Chem. 2006 Sep 29;281(39):29054-63. doi: 10.1074/jbc.M602638200. Epub 2006 Jul 26.
17. Hasegawa M, Osaka T, Tawaratsumida K, Yamazaki T, Tada H, Chen GY, Tsuneda S, Núñez G, Inohara N. Transitions in oral and intestinal microflora composition and innate

immune receptor-dependent stimulation during mouse development. Infect Immun. 2010 Feb;78(2):639-50. doi: 10.1128/IAI.01043-09. Epub 2009 Nov 23.

18. Hochberg Y, Benjamini Y. More powerful procedures for multiple significance testing. Stat Med. 1990 Jul;9(7):811-8. doi: 10.1002/sim.4780090710. PMID: 2218183.
19. Jiao Y, Hasegawa M, Inohara N. The Role of Oral Pathobionts in Dysbiosis during Periodontitis Development. Journal of Dental Research 2014;93:539-546.
20. Jiao Y, Darzi Y, Tawaratsumida K, Marchesan JT, Hasegawa M, Moon H, Chen GY, Núñez G, Giannobile WV, Raes J, Inohara N. Induction of bone loss by pathobiont-mediated Nod1 signaling in the oral cavity. Cell Host Microbe. 2013 May 15;13(5):595-601. doi: 10.1016/j.chom.2013.04.005.
21. Jones RB, Zhu X, Moan E, Murff HJ, Ness RM, Seidner DL, Sun S, Yu C, Dai Q, Fodor AA, Azcarate-Peril MA, Shrubsole MJ. Inter-niche and inter-individual variation in gut microbial community assessment using stool, rectal swab, and mucosal samples. Scientific reports. 2018;8(1):4139.
22. Kitamoto S, Nagao-Kitamoto H, Jiao Y, Gillilland MG 3rd, Hayashi A, Imai J, Sugihara K, Miyoshi M, Brazil JC, Kuffa P, Hill BD, Rizvi SM, Wen F, Bishu S, Inohara N, Eaton KA, Nusrat A, Lei YL, Giannobile WV, Kamada N. The Intermucosal Connection between the Mouth and Gut in Commensal Pathobiont-Driven Colitis. Cell. 2020 Jul 23;182(2):447-462.e14.
23. Lalla E, Lamster IB, Hofmann MA, Bucciarelli L, Jerud AP, Tucker S, Lu Y, Papapanou PN, Schmidt AM. Oral infection with a periodontal pathogen accelerates early atherosclerosis in apolipoprotein E-null mice. Arterioscler Thromb Vasc Biol. 2003 Aug 1;23(8):1405-11.
24. Mahendran S, Vijayabaskar P, Saravanan S, Anandapandian KTK, Shank T. Structural characterization and biological activity of exopolysaccharide from Lysinibacillus fusiformis. African Journal of Microbiology Research 2013;7:4629-4639
25. Marchesan J, Girnary MS, Jing L, Miao MZ, Zhang S, Sun L, Morelli T, Schoenfisch MH, Inohara N, Offenbacher S, Jiao Y. An experimental murine model to study periodontitis. Nat Protoc. 2018 Oct;13(10):2247-2267.
26. Marchesan J, Jiao Y, Schaff RA, et al. TLR4, NOD1 and NOD2 mediate immune recognition of putative newly identified periodontal pathogens. Molecular oral microbiology 2016;31:243-258.
27. Marchesan JT, Morelli T, Lundy SK, Jiao Y, Lim S, Inohara N, Nunez G, Fox DA, Giannobile WV. Divergence of the systemic immune response following oral infection with distinct strains of Porphyromonas gingivalis. Mol Oral Microbiol. 2012 Dec;27(6):483-95.
28. Marchesan JT, Gerow EA, Schaff R, Taut AD, Shin SY, Sugai J, Brand D, Burberry A, Jorns J, Lundy SK, Nuñez G, Fox DA, Giannobile WV. Porphyromonas gingivalis oral infection exacerbates the development and severity of collagen-induced arthritis. Arthritis Res Ther. 2013 Nov 12;15(6):R186.
29. Niazi SA, Clarke D, Do T, Gilbert SC, Mannocci F, Beighton D. Propionibacterium acnes and Staphylococcus epidermidis isolated from refractory endodontic lesions are opportunistic pathogens. J Clin Microbiol. 2010;48(11):3859–3869.

30. Nociti FH, Jr., Casati MZ, Duarte PM. Current perspective of the impact of smoking on the progression and treatment of periodontitis. Periodontol 2000 2015;67:187-210.
31. Okuda, K., Kato, T., Shiozu, J., Takazoe, I., and Nakamura, T. Bacteroides heparinolyticus sp. nov. isolated from humans with periodontitis. Int. J. Syst. Bacteriol. (1985) 35:438-442.
32. Paes Batista da Silva A, Barros SP, Moss K, et al. Microbial Profiling in Experimentally Induced Biofilm Overgrowth Among Patients With Various Periodontal States. Journal of Periodontology 2016;87:27-35.
33. Palmer RJ Jr, Shah N, Valm A, Paster B, Dewhirst F, Inui T, Cisar JO. Interbacterial Adhesion Networks within Early Oral Biofilms of Single Human Hosts. Appl Environ Microbiol. 2017 May 17;83(11):e00407-17.
34. Paster BJ, Boches SK, Galvin JL, et al. Bacterial diversity in human subgingival plaque. J Bacteriol 2001;183:3770-3783.
35. Sanz M, Ceriello A, Buysschaert M, et al. Scientific evidence on the links between periodontal diseases and diabetes: Consensus report and guidelines of the joint workshop on periodontal diseases and diabetes by the International Diabetes Federation and the European Federation of Periodontology. Journal of Clinical Periodontology 2018;45:138-149.
36. Sato K, Yamazaki K, Kato T, Nakanishi Y, Tsuzuno T, Yokoji-Takeuchi M, Yamada-Hara M, Miura N, Okuda S, Ohno H, Yamazaki K. Obesity-Related Gut Microbiota Aggravates Alveolar Bone Destruction in Experimental Periodontitis through Elevation of Uric Acid. mBio. 2021 Jun 29;12(3):e0077121.
37. Socransky SS, Manganiello AD, Propas D, Oram V, van Houte J. Bacteriological studies of developing supragingival dental plaque. J Periodontal Res. 1977 Mar;12(2):90-106.
38. Souto R, Colombo AP. Prevalence of Enterococcus faecalis in subgingival biofilm and saliva of subjects with chronic periodontal infection. Arch Oral Biol. 2008 Feb;53(2):155-60. doi: 10.1016/j.archoralbio.2007.08.004. Epub 2007 Sep 25. PMID: 17897617.
39. Souto R, Silva-Boghossian CM, Colombo AP. Prevalence of Pseudomonas aeruginosa and Acinetobacter spp. in subgingival biofilm and saliva of subjects with chronic periodontal infection. Braz J Microbiol. 2014;45(2):495-501.
40. Swanson KV, Girnary M, Alves T, Ting JP, Divaris K, Beck J, Pucinelli CM, da Silva RAB, Uyan D, Wilson JE, Seaman WT, Webster-Cyriaque J, Vias N, Jiao Y, Cantley L, Marlier A, Arnold RR, Marchesan JT. Interferon activated gene 204 (Ifi204) protects against bone loss in experimental periodontitis. J Periodontol. 2022 Apr 11.
41. Szafranski SP, Wos-Oxley ML, Vilchez-Vargas R, Jáuregui R, Plumeier I, Klawonn F, Tomasch J, Meisinger C, Kühnisch J, Sztajer H, Pieper DH, Wagner-Döbler I. High-resolution taxonomic profiling of the subgingival microbiome for biomarker discovery and periodontitis diagnosis. Appl Environ Microbiol. 2015 Feb;81(3):1047-58.
42. Teles FR, Teles RP, Uzel NG, Song XQ, Torresyap G, Socransky SS, Haffajee AD. Early microbial succession in redeveloping dental biofilms in periodontal health and disease. J Periodontal Res. 2012 Feb;47(1):95-104.
43. Teles F, Wang Y, Hajishengallis G, Hasturk H, Marchesan JT. Impact of systemic factors in shaping the periodontal microbiome. Periodontol 2000. 2021;85(1):126-160.

44. Thompson AL, Monteagudo-Mera A, Cadenas MB, et al. Milk- and solid-feeding practices and daycare attendance are associated with differences in bacterial diversity, predominant communities, and metabolic and immune function of the infant gut microbiome. Front Cell Infect Microbiol. 2015;5:5.
45. Vieira Colombo AP, Magalhães CB, Hartenbach FA, Martins do Souto R, Maciel da Silva-Boghossian C. Periodontal-disease-associated biofilm: A reservoir for pathogens of medical importance. Microb Pathog. 2016;94:27-34.

FIGURE LEGENDS

Figure 1: Study flowchart of the murine experimental periodontitis induced using the ligature model.

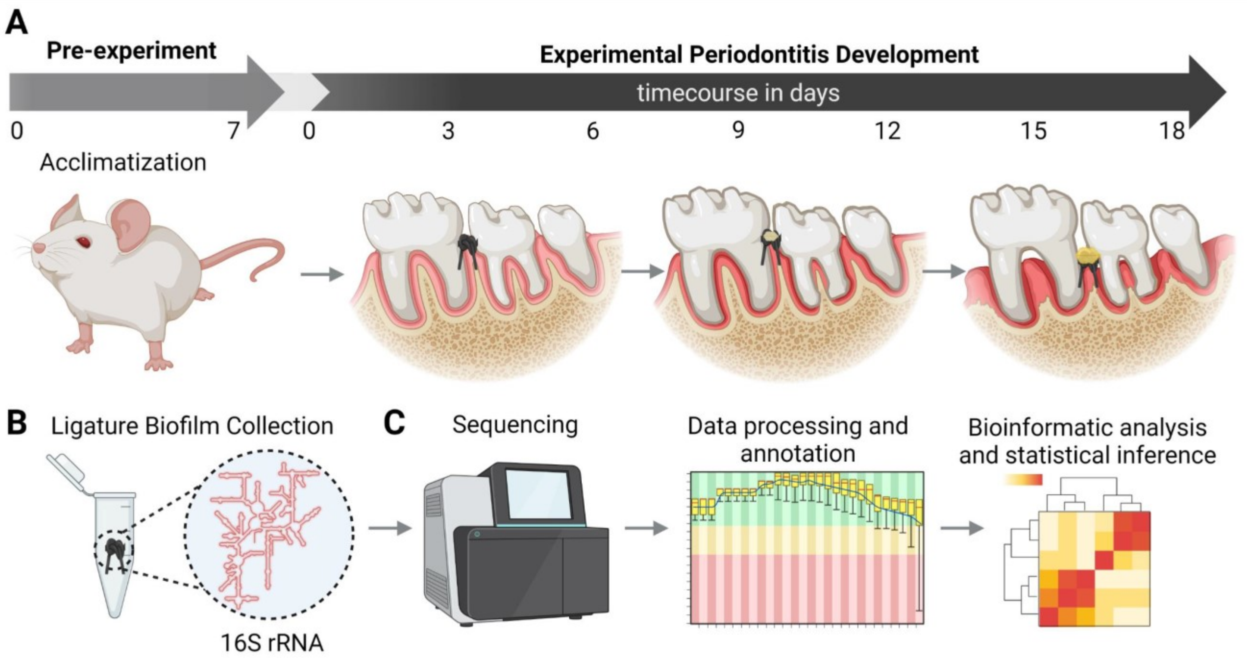

Figure 2: Bacterial microbiome composition shifts according to time. (A) Stacked plot for samples' distribution according to time. For illustrations purposes, only the top 20 genera and species are shown in the plot. The community is represented as 99.2% at day 0, 97.9% at day 3, 87.8% at day 6, 93.9% at day 9, 89.8% at day 12, 92% at day 15, and 82.3% at day 18. (B) Relative abundances (%) of *Lactobacillus, Streptococcus*, and *Enterococcus* during the time course. (C) Species abundance that significantly changed during the time course (Mantel-Haensel test, $p<0.05$, Bonferroni corrected).

Figure 3: Ecological shifts in the microbiome community associated with the length of the ligature presence. (A) Alpha diversity. (B) Unweighted UniFrac Principal Coordinate Analysis (beta diversity) based on time course. (C) Box-plot showing differences between the microbiome communities composition (PERMANOVA, p=0.001).

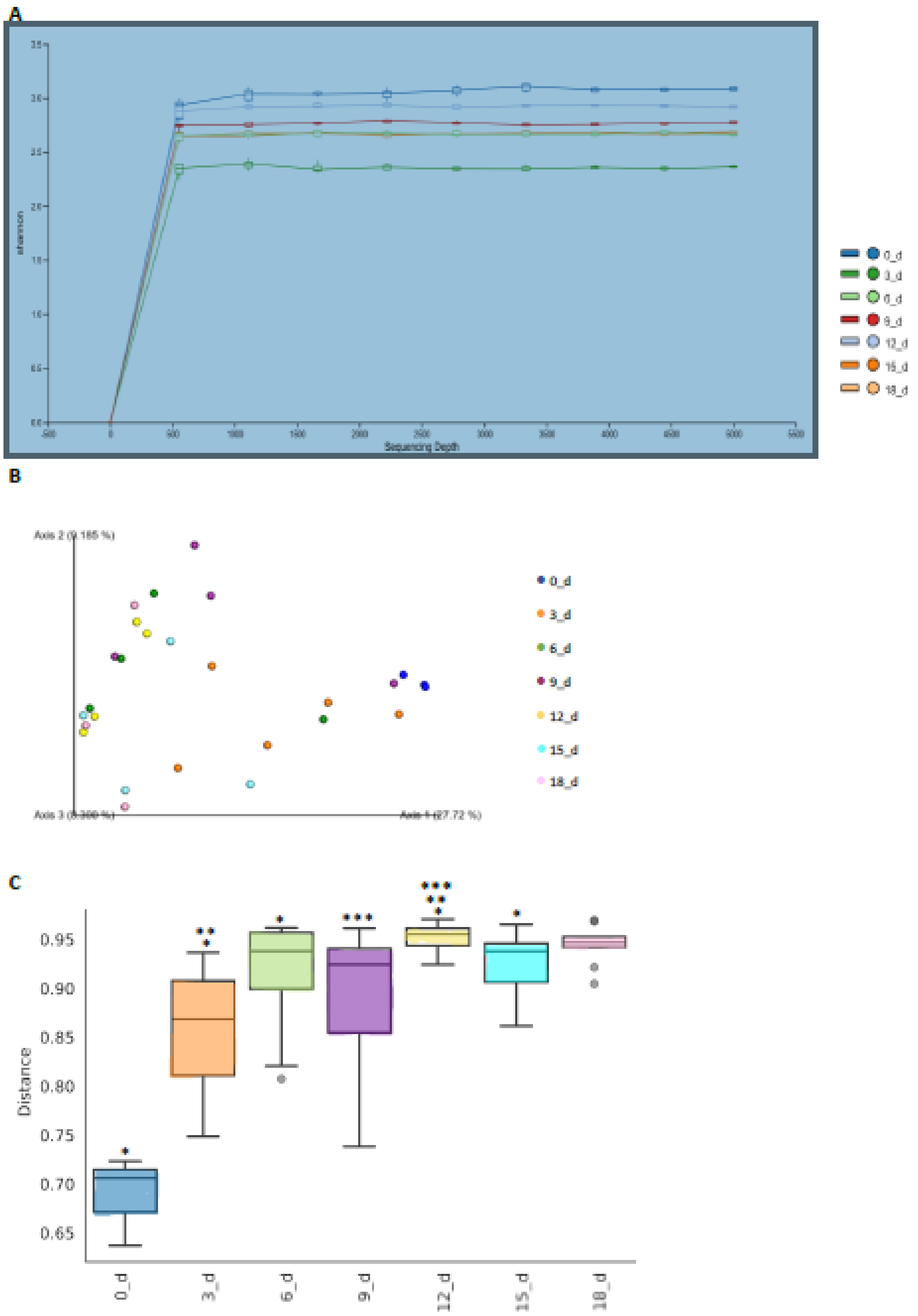

Figure 4: Shift of the bacterial microbiome community at genera level, associated with disease development. (A) Stacked plot for samples' distribution according to clinical diagnosis. (B) Shannon Index: bacterial diversity decreased within samples during disease development. (C) Unweighted UniFrac Principal Coordinate Analysis (Beta diversity) based on periodontal status. (D) Box-plot showing differences between the microbiome communities composition associated with disease development (PERMANOVA, p=0.001).

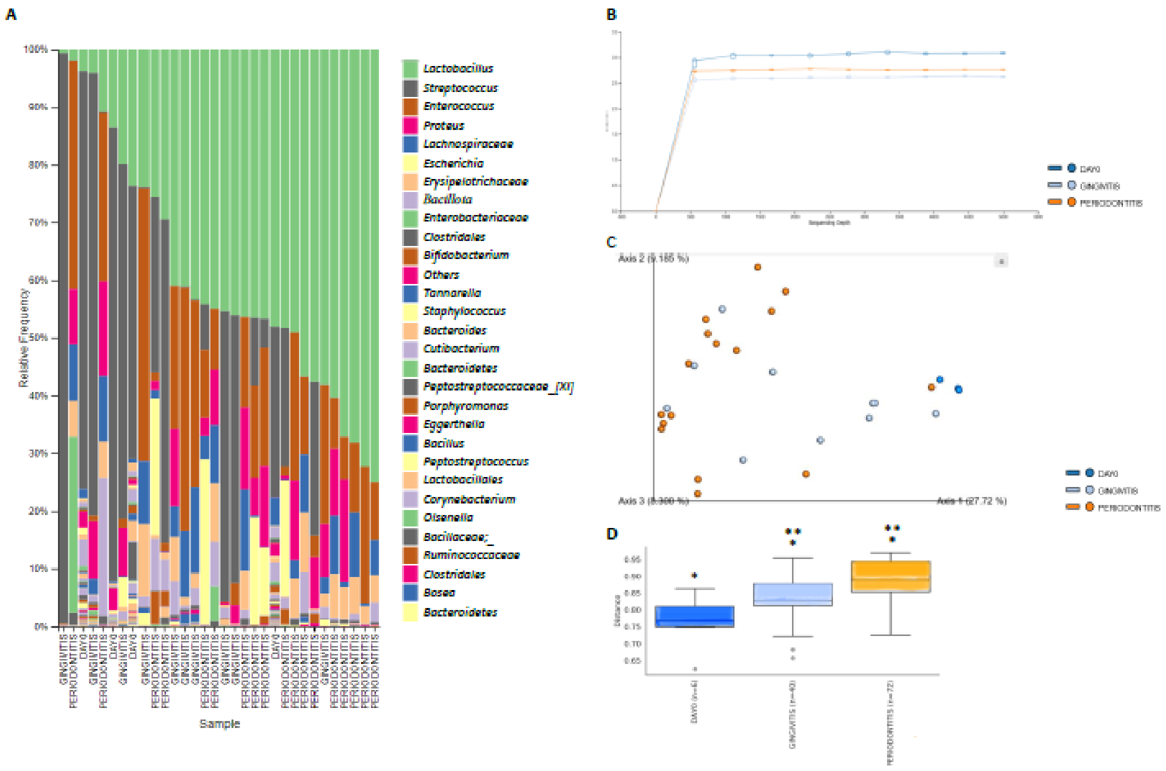

Figure 5: Shift of the bacterial microbiome community associated with disease development. (A) Stacked plot for samples' distribution according to clinical diagnosis. For illustrations purposes, only the top 20 genera and species are shown in the plot. The community is represented as 98% in health, 97.7% in gingival inflammation, and 93.5% in periodontitis. (B) Species abundance that significantly changed associated with periodontal disease progression (Mantel-Haensel test, p<0.05, Bonferroni corrected).

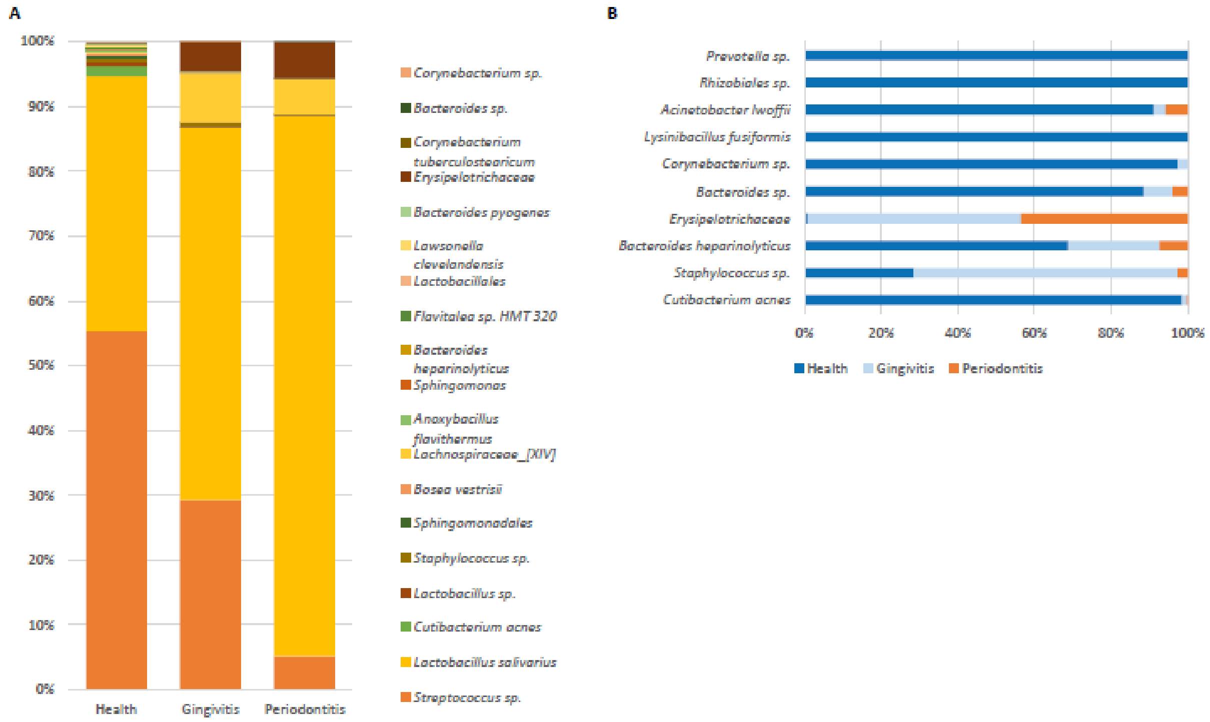

Running title: Oral biofilm microbiome dysbiosis in experimental periodontitis

Word count: 2658

Abstract word count: 350

Summary word count: 250

Tables and Figures: 6 figures

References: 39

Summary

Gingivitis and periodontitis are inflammatory diseases associated with oral biofilm dysbiosis. In this study, we determine the polymicrobial community shifts that occur during the development inflammatory bone loss, by using a murine model of experimental periodontitis induced in C57BL/6 mice and ligature placement. Healthy oral mucosa and ligature biofilm samples were evaluated by 16SrRNA gene sequencing (Illumina MiSeq). Microbial differences between health and periodontal inflammation were observed at all phylogenic levels. An evident microbial community shift occurred in 25 genera during the development of gingival inflammation (3-6d) to periodontal bone loss (9-18d). From day 0-18, dramatic changes were identified in levels of *Streptococcus,* with an overall decrease (54.04-0.02%) as well as levels of *Enterococcus* and *Lactobacillus,* with an

overall increase (23.7-73.1% and 10.1%-70.2%, respectively). Alpha diversity was highest at health (0d) and decreased to its lowest levels at 3d. Beta-diversity increased after ligature placement, indicating that bone loss develops in response to a greater microbial variability (p=0.001). Levels of facultative and strict anaerobic bacteria augmented over the course of the 18d of disease progression. The data suggests that gingival inflammation and bone loss in murine periodontitis develop in response to microbiome shifts. Gingival inflammation is orchestrated by a specific microbiome: alpha diversity was highest at health and decreased to its lowest level at the initial phase of disease, indicating that the microbiome becomes less diverse and, therefore, more specific to the development of periodontal inflammation. These findings support the utilization of the ligature model for microbial shift analysis under different experimental conditions.